

Photoemission and x-ray absorption study of $\text{MgC}_{1-x}\text{Ni}_3$

J. H. Kim¹, J. S. Ahn¹, Jinsoo Kim², Min-Seok Park³, S. I. Lee³, E. J. Choi^{1,2}, and S.-J. Oh^{1,†}

¹*School of Physics and Center for Strongly Correlated Materials Research,
Seoul National University, Seoul 151-742, Republic of Korea*

²*Department of Physics, University of Seoul, Seoul 130-743, Republic of Korea and*

³*National Creative Research Initiative Center for Superconductivity and Department of Physics,
Pohang University of Science and Technology,
Pohang 790-784, Republic of Korea*

We investigated electronic structure of $\text{MgC}_{1-x}\text{Ni}_3$ with photoemission and x-ray absorption spectroscopy. Both results show that overall band structure is in reasonable agreement with band structure calculations including the existence of von Hove singularity (vHs) near E_F . However, we find that the sharp vHs peak theoretically predicted near the E_F is substantially suppressed. As for the Ni core level and absorption spectrum, there exist the satellites of Ni 2*p* which have a little larger energy separation and reduced intensity compared to the case of Ni-metal. These facts indicate that correlation effects among Ni 3*d* electrons may be important to understand various physical properties.

I. INTRODUCTION

Interplay between superconductivity and magnetism is a source of rich solid state physics. In particular, much attention is being paid to the superconductors in close vicinity with ferromagnetism (FM). In Sr_2RuO_4 ¹, the *p*-wave pairing symmetry is thought to be intimately related with the FM fluctuation of Ru ions. In UGe_2 ² and ZrZn_2 ³, the two phases were found to coexist. While it was generally believed that FM and SC are mutually exclusive, these observations suggest that the current understanding needs to be modified.

Recently, following the discovery of superconductivity in MgB_2 ⁴, intermetallic compound $\text{MgC}_{1-x}\text{Ni}_3$ ($x = 0.04 \sim 0.1$)⁵ was reported to be superconducting at $T_c \sim 7\text{K}$. MgCNi_3 has a cubic antiperovskite structure where C is surrounded by six Ni ions to form an octahedral cage. Although the material is paramagnetic at $T > T_c$, Ni ions exhibit ferromagnetic (FM) spin fluctuation as shown by ¹³C NMR experiment⁶. At $T < T_c$, tunneling data⁷ show the zero conductance peak (ZCP) which may suggest a non-*s* wave superconducting gap. These facts seem to indicate that the SC is closely linked with FM in this system, as also discussed theoretically by Rosner *et al.*⁸. On the other hand, the result from specific heat experiment⁹ is consistent with conventional BCS behavior. Also, Shim *et al.*¹⁰ showed that the observed T_c is reasonably explained within the BCS electron-phonon interaction mechanism. Thus, the origin of SC in MgCNi_3 is still controversial.

Studying electronic structure of this material, particularly near the Fermi energy, is essential to understand the SC. Band calculations^{8,10,11} show that the Ni-3*d* state is hybridized with C 2*p*, which dominate density of state (DOS) at E_F . In particular, it is predicted that a van Hove singularity (vHs) peak exist very close to the E_F . The vHs peak gives rise to a large DOS at E_F which can be directly related with the superconductive coupling constant. It is thus important to ex-

perimentally probe the vHs peak in detail. Photoemission spectroscopy (PES) is a powerful tool to investigate energy-band structures and electron correlation effects. In this work, we performed PES and x-ray absorption spectroscopy (XAS) measurements of MgCNi_3 . We find that overall electronic structure is in general agreement with band calculation results. The vHs peak is also identified at about 100 meV below E_F . However, its intensity is much weaker than the theoretical predictions. We discuss several possibilities of the suppression and its implication on the SC.

II. EXPERIMENT

Polycrystalline sample used in this experiment was synthesized by the powder metallurgical technique. Powders were mixed in nominal composition of $\text{Mg}_{1.2}\text{C}_{1.45}\text{Ni}_3$. Here, excess Mg and C were added to maximize carbon incorporation in $\text{MgC}_{1-x}\text{Ni}_3$, similar to the previous report.⁵ The powders were pelletized, wrapped in a Ta foil, and then quartz-sealed under vacuum. The sample was reacted for about two hour at 900 °C and quenched. X-ray diffraction (Rigaku RINT d-max) showed that the sample is in a single phase. Small amount of MgO impurity and some unreacted carbon were also identified. Magnetic susceptibility was measured with a dc SQUID magnetometer (Quantum Design). As shown in Figure 1, the superconducting onset temperature of this as-grown sample was 6.8 K and the transition width measured from 10 ~ 90 % transition was about 0.3 K. These results were close to the previous reports of $\text{MgC}_{1-x}\text{Ni}_3$.⁵ Afterward we put the sample in a high pressure cell and annealed under 3GPa at 900 °C for 30 min¹² to make densified sample for PES and XAS measurements. After this treatment, the pellet density increased significantly and was almost identical to its theoretical value. Figure 1 shows that T_c also increased by about 0.7K and the transition became sharper.

PES experiments were performed using both He I ($h\nu = 21.2$ eV) source at home laboratory and 120 eV photon at Pohang Light Source (PLS) in Korea. Mg K_α line ($h\nu = 1253.6$ eV) was used in x-ray photoemission spectroscopy (XPS). The resolution for He I, 120 eV and Mg K_α are 40 meV, 100 meV and 1eV, respectively. Also, we carried out Ni L_3 -edge XAS at PLS. Samples were *in-situ* fractured to obtain clean surface. Base pressure was 2×10^{-10} torr. For the energy calibration, a bulk palladium was measured at the same time.

III. RESULT AND DISCUSSION

Inset in Figure 2 shows PES data taken with 120 eV photon source. The peak centered at 1eV below E_F corresponds to the Ni $3d$ derived conduction band. After the high pressure (HP) treatment, the spectrum below 3eV decreased substantially. In general, photoemission intensity below the conduction band arises from non-intrinsic sources such as grain boundary or surface contamination. Decrease of it, together with the T_c enhancement, suggests that the sample quality is improved by the HP sintering. Note, however, that the band structure above 3eV is almost independent of the sintering. Afterwards, we show the data of the HP sintered sample. Even the high-pressure sintered sample shows structures around ~ 6 eV binding energy which we presume mostly come from remnant MgO precipitates or grain boundaries. It may also be related with the structural inhomogeneity¹³ and the nanoprecipitates¹⁴ which were recently reported in this system.

To see the spectra near E_F more closely, we took spectrum using He I source (Figure 2, solid circles). For comparison, we also show predicted spectra from the three band calculations by Shim *et al.*¹⁰ (dotted), by Rosner *et al.*⁸ (dash dot) and by Dugdale *et al.*¹¹ (short dot). To get these lines, the theoretical densities of states were first convoluted by the Fermi-Dirac distribution, followed by broadening procedures: the energy-dependent Lorentzian broadening with $\sim \alpha |E - E_F|$ ($\alpha = 0.3$) and the Gaussian instrumental broadening of 40 meV linewidth.¹⁵ The curves were normalized to give the same integrated spectral weight as the experimental data. The short dash-dotted line shows the background based on the Shirley method.

In the data, four features are observed at ~ 2.7 eV, 1.2 eV, 0.7 eV and 0.1 eV. The first three features agree roughly with the theoretical lines, particularly with that by Dugdale¹¹. In the curve by Shim¹⁰, 1.2eV peak position is deeper than the data. The curve by Rosner⁸ doesn't properly predict the structure centered at ~ 1.2 eV. According to band calculations, the three features are from non-bonding Ni $3d$ states.

The peak located very close to E_F (0.1eV) corresponds to the vHs as predicted in the theoretical lines. Note, however, that the peak height is much smaller than the predictions. Rough estimation of the peak intensity

shows about $1/2 \sim 1/4$ of the theoretical peaks. The vHs arise from the saddle point near Γ in the band structure. The peak strength is then determined by the band-curvature or the effective mass at this point. Our observation suggests that the calculations are overestimating the peak intensity or equivalently underestimating the curvature. Also note that the height is different significantly among the three theory results, which shows that band structure near the saddle point depend sensitively on the calculation methods. Thus, correct estimation of the peak strength seems a non-trivial work.

In spite of the uncertainty in the calculation, the observed peak is smaller than any of the three curves. This may suggest that the peak is suppressed for reasons not accounted for in the band theory.¹⁷ For example, when electron-phonon interaction or electron-electron interaction are present, part of spectral weight will shift to higher energy. $\text{YNi}_2\text{B}_2\text{C}$, a superconductor which bears some similarity with MgCNi_3 where Ni-B and Ni-C bondings are important, is another system that has vHs close to E_F . There, the observed peak is also suppressed compared with theoretical prediction and Kobayashi *et al.*¹⁸ interpreted it in terms of electron-electron or electron-phonon interaction.

It is also possible that the spectral weight suppression may be due to matrix element effects.^{19,20} In this case, the peak intensity will depend on the photon energy. We thus performed PES using various photon energy from 40 eV to 150 eV, but the spectra didn't change.²¹ Surface effect to which UPS is somewhat sensitive is another possible source. The vHs is a bulk property which arises from the saddle point (Γ) of the Fermi surface. As one approaches the surface, the band structure will change and the vHs feature may possibly be smeared.²²

Figure 3 shows Ni $2p$ core-level photoemission spectrum of $\text{MgC}_{1-x}\text{Ni}_3$. The main peaks, corresponding to Ni $2p_{3/2}$ and $2p_{1/2}$, respectively, are accompanied by the weak satellites at higher binding energies. The existence of this satellite structure signals the presence of $d-d$ electron correlation effect, since such satellite structure originates from the two-hole bound state. For comparison with related compounds, we show Ni $2p$ spectra of Ni-metal²³ and $\text{YNi}_2\text{B}_2\text{C}$ ¹⁸ together with our data in the inset. Note that in $\text{MgC}_{1-x}\text{Ni}_3$ the satellite position of Ni $2p_{3/2}$ is a little large and its intensity is largely reduced compared with Ni-metal. In the first order approximation, the relative satellite position and the intensity represent the $d-d$ correlation energy and the number of d holes, respectively. Thus our observations imply that the correlation energy is a little farther apart and the d hole number is smaller in $\text{MgC}_{1-x}\text{Ni}_3$ compared with Ni-metal.

In $\text{MgC}_{1-x}\text{Ni}_3$, Ni is strongly covalent bonded with C and then charge transfer from the Ni atoms to C will occur. This will result in the Ni $2p$ core level shift to higher binding energy. The observed shift in $\text{YNi}_2\text{B}_2\text{C}$ is explained in this manner.²⁴ However, the binding energy of Ni $2p$ is almost similar to that of Ni metal. This seems

to suggest that there is a large reduction of the binding energy due to, probably, a screening of core hole by free carriers. In fact, the CNi_3 cage is fully charged by the two electrons donated by the Mg^{+2} ion and thus Ni hole will be effectively screened.

Figure 4 shows Ni L_3 -edge XAS spectrum of $\text{MgC}_{1-x}\text{Ni}_3$. It is compared with the calculated Ni PDOS above the E_F in the band calculation result by Shim *et al.*¹⁰ To get the theoretical curve (dash-dotted line), the Ni partial density of states are broadened by convoluting with the similar way as we did in Figure 2. But in this case we used the Lorentzian broadening with linewidth $\sim \alpha(E - E_F)^2$ ($\alpha = 0.2$) and the Gaussian broadening 1.6 eV . The two curves are normalized to give the same integrated spectral weight. We see that overall structure is in reasonable agreement with the band calculations. The peak just above E_F is due to the unoccupied part of Ni $3d$ band. But we also observe the satellite structures around $h\nu = 863 \text{ eV}$ in the experiments, which represents the correlation effects.

IV. CONCLUSION

In conclusion, we have performed XPS, XAS, and UPS measurements to study the electronic structure of

$\text{MgC}_{1-x}\text{Ni}_3$. The satellite structure seen in Ni $2p$ XPS spectrum suggests that the $3d$ electron correlation is substantial. L_3 -edge XAS and UPS data show that the position and width of the Ni $3d$ derived valence band is in reasonable agreement with theoretical calculation results. The vHs peak is found at $\sim 0.12 \text{ eV}$ below the Fermi energy. Its spectral weight is largely suppressed compared with theoretical predictions and we suggested various possibilities of the suppression including the electron-electron and electron-phonon interaction.

Acknowledgments

We thank H.C. Kim and H.C. Lee for sample characterization at KBSI. We also appreciate K.-J. Kim for the work at PLS. This work was supported by the KOSEF through the CSCMR.

[†] To whom correspondences should be addressed: sjoh@physics.snu.ac.kr. Inquiry for the samples can be made to E. J. Choi: echoi@uoscc.uos.ac.kr

¹ R. Matzdorf *et al.*, Science **289**, 746 (2000).

² S. S. Saxena *et al.*, Nature (London) **406**, 587 (2000).

³ C. Pfeleiderer, M. Uhlarz, S. M. Hayden, R. Vollmer, H. v. Lohneysen, N. R. Bernhoeft, and G. G. Lonzarich, Nature (London) **412**, 58 (2001).

⁴ J. Nagamatsu, N. Nakagawa, T. Muranaka, Y. Zenitani, J. Akimitsu, Nature **410**, 63 (2001).

⁵ T. He, Q. Huang, A. P. Ramirez, Y. Wang, K. A. Regan, N. Rogado, M. A. Hayward, M. K. Haas, J. S. Slusky, K. Inumaru, H. W. Zandbergen, N. P. Ong, and R. J. Cava, Nature **411**, 54 (2001).

⁶ P. M. Singer, T. Imai, T. He, M. A. Hayward, and R. J. Cava, cond-mat/0106476.

⁷ Z. Q. Mao, M. M. Rosario, K. Nelson, K. Wu, I. G. Deac, P. Schiffer, Y. Liu, T. He, K. A. Regan, and R. J. Cava, cond-mat/0105280.

⁸ H. Rosner, R. Weht, M. D. Johannes, W. E. Pickett, and E. Tosatti, Phys. Rev. Lett **88**, 027001 (2002).

⁹ J.-Y. Lin, P. L. Ho, H. L. Huang, P. H. Lin, Y.-L. Zhang, R.-C. Yu, C.-Q. Jin, H. D. Yang, cond-mat/0202034.

¹⁰ J. H. Shim, S. K. Kwon, and B. I. Min, Phys. Rev. B. **64**, 180510 (2001).

¹¹ S. B. Dugdale and T. Jarlborg, Phys. Rev. B **64**, 100508 (2001).

¹² C. U. Jung, Min-Seok Park, W. N. Kang, Num-Seog Kim, Kijoon H. P. Kim, S. Y. Lee, and Sung-Ik Lee, Appl. Phys. Lett. **78** 4157 (2001).

¹³ J. Q. Li, L. J. Wu, L. Li, and Y. Zhu, Phys. Rev. B. **65**,

052506 (2002)

¹⁴ L.D.Cooley *et al.*, cond-mat/0108397.

¹⁵ For the result by Shim¹⁰, different cross sections were taken into account on the PDOS of the elements (Mg, C, and Ni),¹⁶ while the PDOS were not available in the result by Rosner.⁸

¹⁶ J.-J. Yeh and I. Lindau, At. Data Nucl. Data Tables, **32**, 1-155 (1985).

¹⁷ Similar discrepancy between band theory and photoemission data regarding intensities of the narrow peak has been observed before for other SC systems as well. For example, band calculation predicts a narrow peak close to the E_F due to the flat band structure in $\text{BaPb}_{1-x}\text{Bi}_x\text{O}_3$, $\text{Ba}_{1-x}\text{K}_x\text{BiO}_3$, A15 compounds, $\text{Bi}_2\text{Sr}_2\text{CaCu}_2\text{O}_{8+\delta}$, etc. However, photoemission measurements showed that the peak is much suppressed. See for example, H. Namatame *et al.* Phys. Rev. B **48**, 16917 (1993); M. Grioni *et al.*, *ibid.* **43**, 1216 (1991); J.-M. Imer *et al.*, Phys. Rev. Lett. **62**, 336 (1989).

¹⁸ K. Kobayashi, T. Mizokawa, K. Mamiya, A. Sekiyama, A. Fujimori, H. Takagi, H. Eisaki, S. Uchida, R. J. Cava, J. J. Krajewski, and W. F. Peck, Jr., Phys. Rev. B **54**, 507 (1996).

¹⁹ A. Bansil and M. Lindroos, Phys. Rev. B **83**, 5154 (1999)

²⁰ Tschang-Uh Nahm *et al.*, Phys. Rev. Lett **71**, 1419 - 1422 (1993)

²¹ In addition to intrinsic origins, there may be extrinsic factors. Essential inhomogeneity was reported to exist commonly in this superconducting sample.¹³ By analyzing the bulk flux-pinning force curve, Cooley *et al.*¹⁴ reported there is a large fraction of precipitates present in MgCNi_3 .

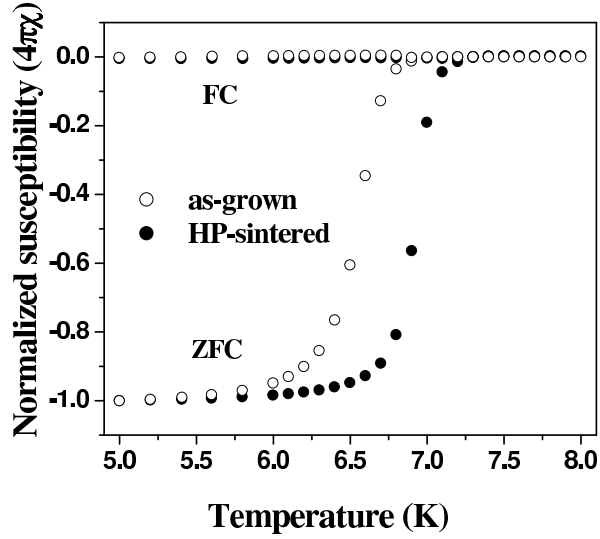
It is possible that these defect structures affect its normal-state and superconducting properties.

²² J. I. Lee, private communication.

²³ *Handbook of X-Ray Photoelectron Spectroscopy*, by J. F. Moulder, W. F. Stickle, P. E. Sobol, and K. D. Bomben, edited by J. Chastain and R. C. King, Jr., (Physical Electronics, Prairie, 1995).

²⁴ E. Pellegrin, G. Meigs, C. T. Chen, R. J. Cava, J. J. Krajewski, and W. F. Peck, Jr., *Phys. Rev. B* **51**, 16159 (1995)

FIG. 1: Normalized magnetic susceptibility from the measured low-field magnetization $M(T, H = 10Oe)$ of as-grown (solid circles) and sintered at 900°C under 3GPa (open circles).



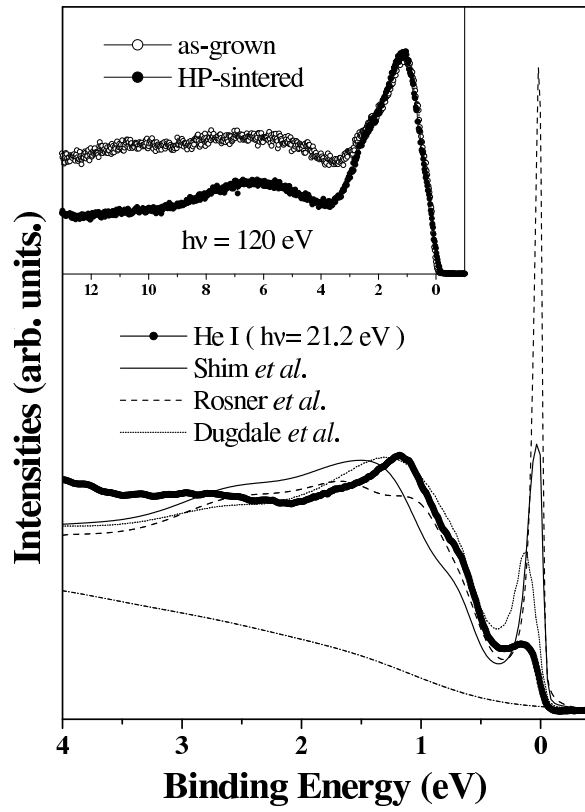


FIG. 2: He I UPS spectrum (\bullet) of $\text{MgC}_{1-x}\text{Ni}_3$ at room temperature. All lines are theoretical spectra derived from the band-structure calculations. The short dash-dotted line shows the background. Inset: Valence region photoemission spectra with photon energy 120 eV of as-grown (solid circles) and sintered at 900°C under 3GPa (open circles).

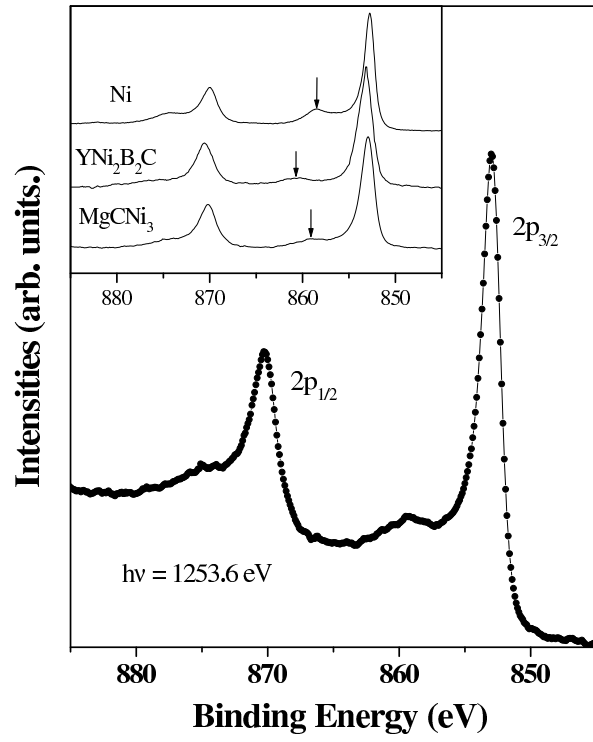


FIG. 3: Ni 2p core-level photoemission spectrum of MgC_{1-x}Ni₃. Inset: Ni 2p spectra of Ni-metal²³ and YNi₂B₂C¹⁸ are compared with that of MgC_{1-x}Ni₃.

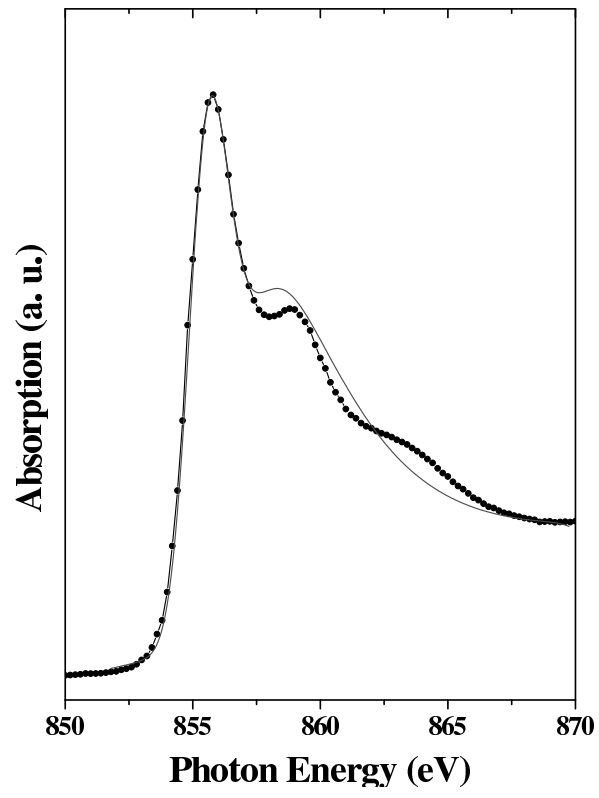


FIG. 4: Ni L_3 -edge XAS spectrum of $\text{MgC}_{1-x}\text{Ni}_3$ (\bullet). The band calculation result (dash-dotted line) by Shim *et al.*¹⁰ is compared. See text for the convolution.